applied optics

Simulation and experimental research of a high-order Bragg grating semiconductor laser

SIYU E,[1,2] YINLI ZHOU,[1,*] XING ZHANG,[1] JIANWEI ZHANG,[1] YUGANG ZENG,[1] JINJIANG CUI,[3,4] YUN LIU,[1] YONGQIANG NING,[1] AND LIJUN WANG[1]

[1]State Key Laboratory of Luminescence and Applications, Changchun Institute of Optics, Fine Mechanics and Physics, Changchun 130033, China
[2]University of Chinese Academy of Sciences, Beijing 100049, China
[3]Suzhou Institute of Biomedical Engineering and Technology, Chinese Academy of Sciences, Suzhou 215163, China
[4]Jinan Guoke Medical Science & Technology Development Co., Ltd, Jinan 250000, China
*Corresponding author: zhouyinli@ciomp.ac.cn

Received 21 May 2021; revised 20 June 2021; accepted 20 June 2021; posted 22 June 2021 (Doc. ID 432175); published 14 July 2021

In this paper, the influence of the epitaxial structure on distributed Bragg reflector (DBR) grating characteristics is studied by simulation analysis. Comparative analysis shows that the symmetrical epitaxial structure can achieve a lower threshold current and, thus, a higher power. Based on the simulated structure, a DBR laser based on a symmetric epitaxial structure was fabricated, and a single longitudinal mode laser output at ∼1060 nm was obtained. The maximum power was 104.5 mW, and the side mode suppression ratio (SMSR) is 43 dB.

https://doi.org/10.1364/AO.432175

1. INTRODUCTION

Narrow linewidth semiconductor lasers are widely used in space optical communications [1], precision measurement [2], pumping solid-state lasers, and optical fibers [3] due to their excellent spectral and coherence characteristics. There are three main types of single-frequency narrow linewidth semiconductor lasers. The first one is an index-coupled distributed feedback laser (DFB) laser, which is prepared by etching low-order gratings and secondary epitaxy [4,5]. DFB lasers can achieve an output power of several hundred milliwatts (mW) and a linewidth of several megahertz (MHz). The second method is a gain-coupled DFB laser [6], which is a single-frequency laser obtained by fabricating periodic electrodes to modulate the light field. The fabrication process of gain-coupled DFB lasers is relatively simple while facing the problem of optical mode instability. It can achieve an output power of hundreds of mW and linewidth of hundreds of MHz. The third one is the distributed Bragg reflector (DBR) laser, which is prepared by etching the periodic grating structure once with a simple process and stable spectral mode. The output power of a single transverse mode (with a ridge width less than 5 microns) a DBR semiconductor laser can reach to 200 mW [7–9]. To further increase the power, various schemes have been adopted, including the use of wide bars that increases the power to 500 mW [10], and the introduction of tapered amplifiers that increases the power to 6 W [11,12].

High-order DBR grating lasers can be prepared only with the help of ordinary lithography machines; on the other hand, high-order gratings suffer from greater light scattering loss. Therefore, optimizing the grating parameters is necessary to improve the laser performance. Many studies provided detailed analyses on high-order gratings [13–16]. Most studies have reported the influence of grating parameters in asymmetric epitaxial structures on the spectral characteristics [17,18]. There have been few studies done on symmetric epitaxial structures. In this paper, the effects of symmetric and asymmetric epitaxial structures on the performance of DBR lasers are compared by simulation analysis. The analysis results show that the DBR laser with a symmetric epitaxial structure makes it easier to obtain high grating reflectivity and suitable FWHM of the reflection spectrum of ∼3 nm [19]. The symmetric epitaxial structure also helps to obtain high mode gain, thus reducing the threshold current of the device. Based on the analysis conclusion, a high-order DBR semiconductor laser with a symmetric epitaxial structure and a ridge width of ∼5 μm was prepared through experiments. The DBR gratings of the device can provide ∼8.3 % grating reflectivity and close to zero light transmittance, so the rear surface of the device does not need anti-reflection coating, which further simplifies the preparation process. The device achieves a high-power, single longitudinal mode and single transverse mode laser output, with a maximum power of 104.5 mW (@ 700 mA) and a side mode suppression ratio (SMSR) of 43 dB.

2. STRUCTURAL DESIGN

We first use the finite element method (FEM) to analyze the light field of the epitaxial structure and combine the two methods of the FEM and the 2D scattering matrix method

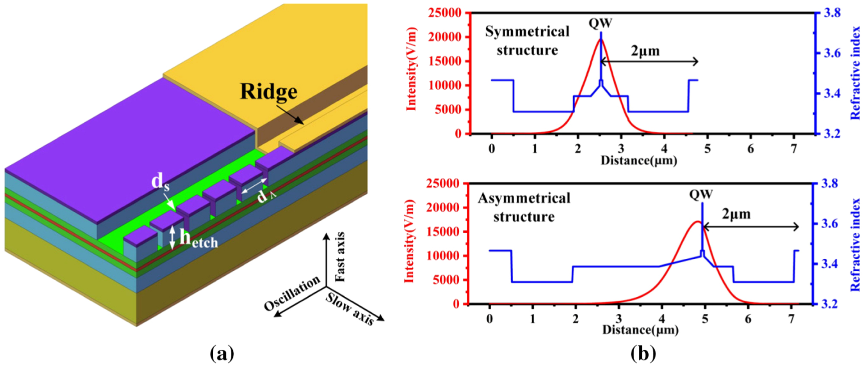

Fig. 1. (a) 3D cross-section drawn along the optical oscillation direction of the DBR laser. (b) Electric field intensity and refractive index distribution along the epitaxial direction of the symmetrical and asymmetrical structure.

(SMM) to simulate the performance of the DBR grating. Using COMSOL software, the influence of the epitaxial structure and a grating parameter on the spectral characteristics of the DBR laser was studied by FEM. Then, the SMM was used to calculate the characteristics of multiple grating pairs [20].

The 3D cross-section of the grating region of the device is shown in Fig. 1(a). The cavity length of the device is 3 mm, and the ridge is 5 μm to maintain a single transverse mode operation. The grating region has no metal electrodes and the length is ~110 μm. The grating parameters include grating period d_Λ, slot width d_s, etching depth h_{etch}, and the grating pairs N. This paper mainly compares the effects of the grating parameters on the spectral characteristics when different epitaxial structures are used. Figure 1(b) shows the optical field and refractive index distribution of the two epitaxial structures.

The definition of the confinement factor is the ratio of the radiant energy confined in the central layer to the total radiant energy produced by the laser, which can be calculated by Eq. (1), where a represents the thickness of the desired layer and b represents the thickness of the entire epitaxial structure. In theory, the larger the ratio, the better the performance of the final laser. The waveguide thickness of the symmetric epitaxial structure is set to 1.2 μm, and the quantum well is located at the center of the light field. The optical confinement factor of the quantum well layer is 0.86%. The asymmetric epitaxial structure contains 2.9 μm N waveguide layer and 0.8 μm P waveguide layer, respectively. The optical confinement factor of the quantum well layer is 0.4%:

$$\Gamma = \int_0^a |E_\tau|^2 \mathrm{d}\tau \Big/ \int_0^b |E_\tau|^2 \mathrm{d}\tau. \qquad \textbf{(1)}$$

Figure 2 shows the effect of slot widths d_s of the two epitaxial structures on the reflection spectrum. It can be seen that, for each structure, the reflectivity has a negative correlation with the d_s, the FWHM of the reflection spectrum hardly changes with d_s, and the position of the reflectivity peak shift blue with an increase of d_s. A comparative analysis shows that the Bragg grating with a symmetric epitaxial structure has a higher reflectivity, a wider FWHM of the reflection spectrum, and a larger reflection peak position that moves as the d_s increases.

The influence of the etching depths h_{etch} of the two epitaxial structures on the reflection spectrum is depicted in Fig. 3. The etching depth is positively correlated with the reflectivity and

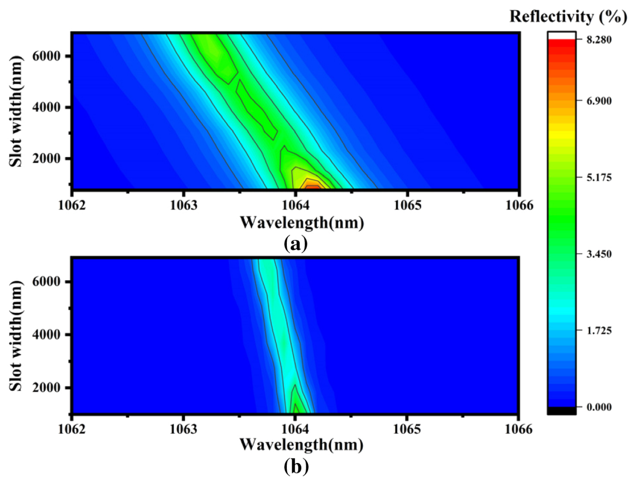

Fig. 2. Variation of Bragg grating reflection spectrum with slot width of (a) the symmetrical epitaxial structure and (b) the asymmetrical epitaxial structure. N is set to 200.

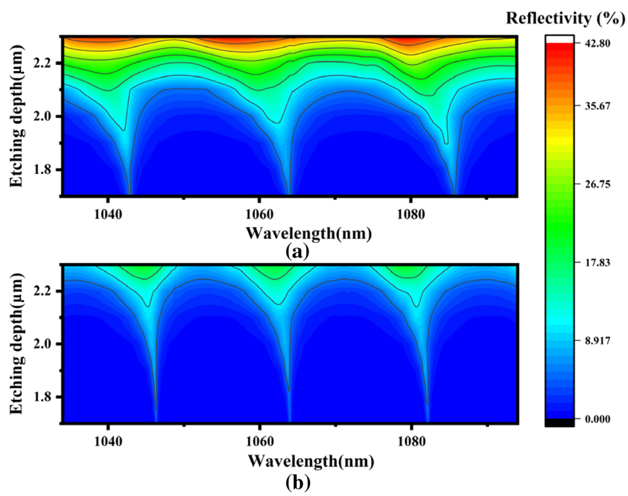

Fig. 3. Variation of Bragg grating reflection spectrum with slot depth of (a) the symmetrical epitaxial structure and (b) the asymmetrical epitaxial structure. N is set to 200.

the FWHM of the reflection spectrum and has a small effect on the reflectivity peak position. Under the same etching depth, the symmetric structure has a higher reflectivity and wider FWHM

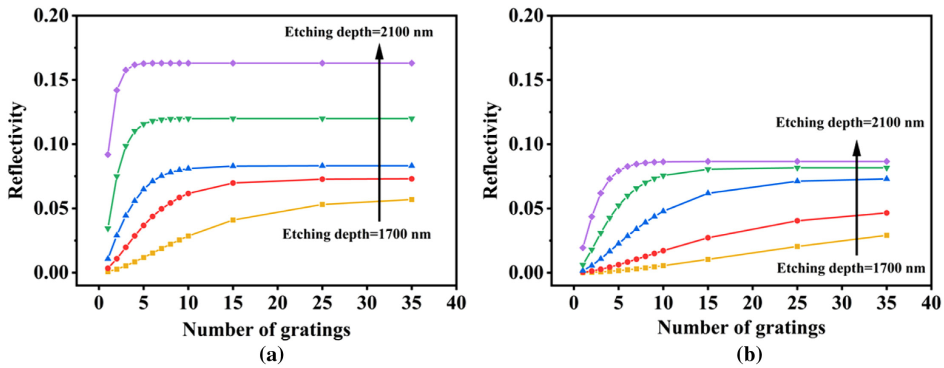

Fig. 4. Variation of Bragg grating reflection spectrum with the number of gratings N under different etching depths of (a) the symmetrical epitaxial structure and (b) the asymmetrical epitaxial structure.

of the reflection spectrum than the asymmetric structure. The grating of the symmetric structure can obtain an optimal reflectivity of $\sim 8.3\,\%$ and FWHM of the reflection spectrum of ~ 3 nm at an etching depth of 1900 nm. To achieve the same effect, the etching depth of the asymmetric epitaxial structure is 2100 nm, which exceeds the location of the quantum well and will introduce the surface defects to form nonradiative recombination centers, thus increasing the optical loss.

Finally, the dependence of the optical spectrum on the numbers of gratings N of the two structures is compared. The variation of reflectivity versus N at different etching depths is shown in Fig. 4. The reflectivity increases rapidly to a maximum as N increases and then remains constant. The symmetrical epitaxial structure can achieve higher reflectivity than the asymmetrical epitaxial structure at the same etching depth and N .

According to the comparative analysis above, it can be concluded that the gratings based on the two epitaxial structures can both achieve the optimal spectral characteristics by selecting the grating parameter combination, respectively. However, the symmetric epitaxial structure does not need to be etched through the quantum well, and only the shallow etching depth can achieve the optimal grating effect, which helps to minimize the light absorption caused by etching. Moreover, the symmetric epitaxial structure also helps to obtain a high mode gain, thereby reducing the threshold current of the device and increasing the photoelectric conversion efficiency. Therefore, a high-order grating DBR laser with a symmetric epitaxial structure is fabricated. A 49-order Bragg grating including a grating period of 7681 nm, a slot width of 1500 nm, an etching depth of 1900 nm, and grating number of 15 is adopted for a sufficiently high grating reflectivity of 8.3 % and an appropriate FWHM of the reflection spectrum of 3 nm. The structural parameters of the device are shown in Table 1.

Table 1. Device Structure Parameters

Waveguide layer thickness	1.2 μm
Ridge width	5 μm
Length of grating area	110 μm
Grating period	7681 nm
Slot width	1500 nm
Etching depth	1900 nm
Pairs of gratings	15

3. FABRICATION AND EXPERIMENTAL RESULTS

The epitaxial structure of the DBR lasers was grown by an AIXTRON 200-4 MOCVD system on an n-GaAs (001) substrate. The active region consists of a layer of $In_{0.25}Ga_{0.75}As/GaAs$ quantum well (QW) with a gain peak position at ~ 1050 nm . The thickness of the symmetric waveguide is 1.2 μm and is doped with Si and Zn as a donor and recipient, respectively. Laser diodes with a 5 μm ridge width were fabricated by conventional lithography. The SiO_2 insulating layer was grown by plasma-enhanced chemical vapor deposition (PECVD). The grating and ridge were fabricated by two lithography and dry etching processes. Ti/Pt/Au and Ni/Ge/Au/Ni/Au ohmic contacts were evaporated on the top and back of the wafer, respectively. After the alloying process, the wafers were cleaved into $3\ \mathrm{mm} \times 500\ \mu\mathrm{m}$ individual chips and then mounted on a standard aluminum nitride heat sink by flip-chip bonding.

Figure 5 shows the spectral characteristics of DBR lasers under different injection currents. When the current varies from 100 mA to 770 mA, the device can maintain single-mode operation and the lasing peak shifts from 1058 nm to 1061 nm. The threshold current and slope efficiencies are 100 mA and 0.14 W/A, respectively. The injection current adjustment factor is ~ 0.003 nm/mA . There is a mode jump at 350 mA and 370 mA; the main reason is that the Bragg frequency determined by the grating and the resonant frequency of the resonant cavity varies with the temperature and injection current [8]. The laser mode jumps to longer wavelengths as the current increases because the gain peak on the long wavelength side of the loss valley determined by the grating [21]. With an increase in the injection current and temperature, the gain peak moves toward a long wavelength, while the loss valley is almost unchanged. This leads to an increase in the difference between the gain and loss, so a bigger injection current is needed to reach the threshold conditions. The device temperature will increase with an increase in the injection current, which causes the laser mode to eventually jump to a longer wavelength. Figure 6 shows the P-I characteristics of the DBR laser at a temperature of 290 K. The maximum output power is 104.5 mW (@ 700 mA). The SMSR at all currents exceeds 30 dB, and the maximum it can reach is 43 dB (@ 330 mA).

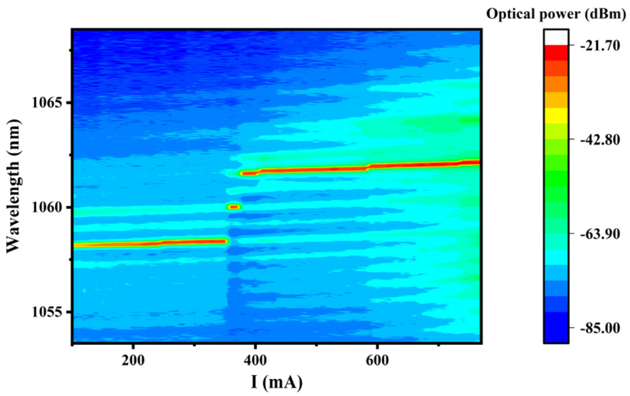

Fig. 5. Spectrogram of different injection currents.

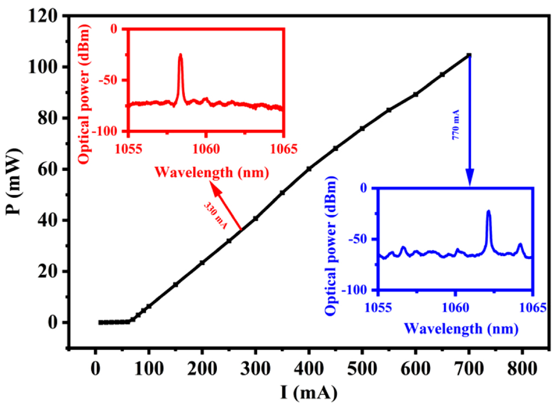

Fig. 6. Relationship between the injected current and output power. Upper left illustration shows the spectrum at 330 mA, and the lower right illustration shows the spectrum at 770 mA.

4. CONCLUSION

In conclusion, the effects of different epitaxial structures on the grating characteristics of high-order DBR lasers are compared in this paper. A symmetric epitaxial structure is helpful to obtain a lower loss and higher mode gain, which is beneficial for the devices to achieve a low threshold and high efficiency. High-order grating DBR lasers with symmetric epitaxial structures are prepared using a set of designed optimal grating parameters. A stable single-mode laser outputting at ∼1060 nm was achieved. The maximum output power and the maximum SMSR are 104.5 mW and 43 dB, respectively.

Funding. Science and Technology Development Project of Jilin Province (20200401006GX); National Natural Science Foundation of China (11774343, 61804151, 61874117, 61874119, 62090060); National Key Research and Development Program of China (2020YFC2200300).

Disclosures. The authors declare no conflicts of interest.

Data Availability. Data underlying the results presented in this paper are not publicly available at this time but may be obtained from the authors upon reasonable request.

REFERENCES

1. Z. Sodnik, B. Furch, and H. Lutz, "Optical intersatellite communication," IEEE J. Sel. Top. Quantum Electron. **16**, 1051–1057 (2010).
2. M. Takamoto, F. Hong, R. Higashi, and H. J. N. Katori, "An optical lattice clock," Nature **435**, 321–324 (2005).
3. S. Zlatanovic, J. S. Park, S. Moro, J. Boggio, I. B. Divliansky, N. Alic, S. Mookherjea, and S. J. N. P. Radic, "Mid-infrared wavelength conversion in silicon waveguides using ultracompact telecom-band-derived pump source," Nat. Photonics **4**, 561–564 (2010).
4. J. Fricke, J. Decker, A. Maassdorf, H. Wenzel, G. Erbert, A. Knigge, and P. Crump, "DFB lasers with apodized surface gratings for wavelength stabilization and high efficiency," Semicond. Sci. Technol.**32**, 075012 (2017).
5. H. Wenzel, J. Fricke, J. Decker, P. Crump, and G. Erbert, "High-power distributed feedback lasers with surface gratings: theory and experiment," IEEE J. Sel. Top. Quantum Electron. **21**, 1502707 (2015).
6. K. Dridi, A. Benhsaien, J. Zhang, and T. J. Hall, "Narrow linewidth 1550 nm corrugated ridge waveguide DFB lasers," IEEE Photon. Technol. Lett. **26**, 1192–1195 (2014).
7. H. Virtanen, A. T. Aho, J. Viheriala, V.-M. Korpijarvi, T. Uusitalo, M. Koskinen, M. Dumitrescu, and M. Guina, "Spectral characteristics of narrow-linewidth high-power 1180 nm DBR laser with surface gratings," IEEE Photon. Technol. Lett. **29**, 114–117 (2017).
8. S. Spießberger, M. Schiemangk, A. Wicht, H. Wenzel, G. Erbert, and G. Tränkle, "DBR laser diodes emitting near 1064 nm with a narrow intrinsic linewidth of 2 kHz," Appl. Phys. B**104**, 813–818 (2011).
9. K. Paschke, J. Pohl, D. Feise, G. Blume, and G. Erbert, "Properties of 62x nm red-emitting single-mode diode lasers," Proc. SPIE **9002**, 90020A (2014).
10. J. J. Coleman, N. L. Dias, and U. Reddy, and IEEE, "Narrow spectral linewidth surface grating DBR diode lasers," in *23rd IEEE International Semiconductor Laser Conference* (IEEE, 2012), pp. 173–174.
11. J. Decker, P. Crump, J. Fricke, A. Maassdorf, G. Erbert, and G. Trankle, "Narrow stripe broad area lasers with high order distributed feedback surface gratings," IEEE Photon. Technol. Lett. **26**, 829–832 (2014).
12. A. Muller, C. Zink, J. Fricke, F. Bugge, O. Brox, G. Erbert, and B. Sumpf, "1030 nm DBR tapered diode laser with up to 16 W of optical output power," Proc. SPIE **10123**, 101231B (2017).
13. Q. Y. Lu, W. H. Guo, R. Phelan, D. Byrne, J. F. Donegan, P. Lambkin, and B. Corbett, "Analysis of slot characteristics in slotted single-mode semiconductor lasers using the 2-D scattering matrix method," IEEE Photon. Technol. Lett. **18**, 2605–2607 (2006).
14. A. Abdullaev, Q. Lu, W. Guo, M. Nawrocka, F. Bello, J. O'Callaghan, and J. F. Donegan, "Linewidth characterization of integrable slotted single-mode lasers," IEEE Photon. Technol. Lett. **26**, 2225–2228 (2014).
15. F. Bello, A. Abdullaev, M. Wallace, M. Nawrocka, Q. Y. Lu, W. H. Guo, and J. F. Donegan, "Traveling wave analysis for a high-order grating, partially slotted laser," IEEE J. Quantum Electron. **51**, 2200305 (2015).
16. B. Mason, G. A. Fish, S. P. DenBaars, and L. A. Coldren, "Widely tunable sampled grating DBR laser with integrated electroabsorption modulator," IEEE Photon. Technol. Lett. **11**, 638–640 (1999).
17. R. K. Price, J. J. Borchardt, V. C. Elarde, R. B. Swint, and J. Coleman, "Narrow-linewidth asymmetric cladding distributed Bragg reflector semiconductor lasers at 850 nm," IEEE Photon. Technol. Lett.**18**, 97–99 (2005).
18. B. Sumpf, K. H. Hasler, P. Adamiec, F. Bugge, J. Fricke, P. Ressel, H. Wenzel, G. Erbert, and G. Traenkle, "1060 nm DBR tapered lasers with 12 W output power and a nearly diffraction limited beam quality," Proc. SPIE**7230**, 72301E (2009).
19. Q. Lu, W.-H. Guo, D. Byrne, and J. F. Donegan, "Design of slotted single-mode lasers suitable for photonic integration," IEEE Photon. Technol. Lett. **22**, 787–789 (2010).
20. S. E, Y. Zhou, X. Zhang, J. Zhang, Y. Huang, Y. Zeng, J. Cui, Y. Liu, Y. Ning, and L. Wang, "High-order DBR semiconductor lasers: effect of grating parameters on grating performance," Appl. Opt.**59**, 8789–8792 (2020).
21. D. Hofstetter and H. P. Zappe, "Anomalous longitudinal mode hops in GaAs/AlGaAs distributed Bragg reflector lasers," Appl. Phys. Lett.**71**, 181–183 (1997).